Dalton Trans., 2016, 45, 561–571. doi: 10.1039/c5dt03758a

Ruthenium Olefin Metathesis Catalysts Featuring Unsymmetrical N-Heterocyclic Carbenes

Veronica Paradiso,[†] Valerio Bertolasi,[‡] Chiara Costabile[†] and Fabia Grisi*[†]

[†]Dipartimento di Chimica e Biologia "Adolfo Zambelli", Università di Salerno, Via Giovanni Paolo II 132, I-84084 Fisciano, Salerno, Italy

[‡]Dipartimento di Chimica and Centro di Strutturistica Diffrattometrica, Università di Ferrara, Via L. Borsari 46, I-44100 Ferrara, Italy

Corresponding author: fgrisi@unisa.it

Abstract

New ruthenium Grubbs'- and Hoveyda- Grubbs' second generation catalysts bearing *N*-alkyl/*N*-isopropylphenyl N-heterocyclic carbene (NHC) ligands with *syn* or *anti* backbone configuration were obtained and compared in model olefin metathesis reactions. Different catalytic efficiency were observed depending on the size of the *N*-alkyl group (methyl or cyclohexyl) and on the backbone configuration. The presence of an *N*-cyclohexyl substituent determined the most significant reactivity differences between catalysts with *syn* or *anti* phenyl groups on the backbone. In particular, *anti* catalysts revealed highly efficient, especially in the ring-closing metathesis (RCM) of encumbered diolefins, while *syn* catalysts showed low efficiency in the RCM of less hindered diolefins. This peculiar behavior, rationalized through DFT studies, was found as related to the high propensity of these catalyst to give nonproductive metathesis events. Enantiopure *anti* catalysts were also tested in asymmetric metathesis reactions, where moderate enantioselectivity was observed. Steric and electronic properties of unsymmetrical NHCs with the *N*-cyclohexyl group were then evaluated using the corresponding rhodium complexes. While steric factors resulted as unimportant for both *syn* and *anti* NHCs, a major electron-donating character was found for the unsymmetrical NHC with *anti* phenyl substituents on the backbone.

Dalton Trans., 2016, 45, 561–571. doi: 10.1039/c5dt03758a

Introduction

Since their introduction in the 1960s,[1] N-heterocyclic carbenes (NHCs) have gained increasingly importance in modern chemistry, with several applications in a large variety of research areas. Their steric and electronic properties make them excellent ancillary ligands for metal catalysts as well as effective organocatalysts. The majority of applications of NHCs, however, are related to their coordination to transition metals, thanks to which efficient catalysts for a huge number of academically and industrially important processes have been found. Indeed, the strong σ-donor capability of NHCs, combined with a shielding steric pattern, leads to increased metal complex stability and improved catalytic activity.[2]

One of the most important and extensively studied transformations mediated by NHC-metal complexes is ruthenium-catalyzed olefin metathesis.[3] The employment of NHC-stabilized ruthenium complexes (second generation catalysts) has given strong impetus to the development of this methodology, which nowadays represents an indispensable synthetic tool for both organic and polymer chemists.[4] Indeed, the use of NHCs as ligands for ruthenium olefin metathesis has given access to unprecedented reactivity pathways and allowed significant advancements in a multitude of challenging reactions.[5-7]

Most of the efforts in designing new ruthenium catalysts involves manipulation of the NHC scaffold of the commercial available second generation catalysts.[8] Indeed, the fine tuning of steric and electronic properties of the NHC ligand can strongly influences catalytic behavior of the resulting ruthenium complexes. The development of unsymmetrical NHCs (uNHCs), able to differentiate steric bulkiness in proximity of the carbenic center, has led to important effects on reactivity and selectivity of the resulting catalysts.[9] Among the numerous examples of ruthenium catalysts presenting uNHCs, those characterized by *N*-alkyl/*N*-aryl substituents have attracted much attention (Chart 1).[10] The major breakthrough in this field is represented by the introduction of a

Dalton Trans., 2016, 45, 561–571. doi: 10.1039/c5dt03758a

series of highly *Z*-selective ruthenium catalysts, incorporating a bidentate unsymmetrical NHC ligand, by the Grubbs group **(4**, Chart 1**)**.[11]

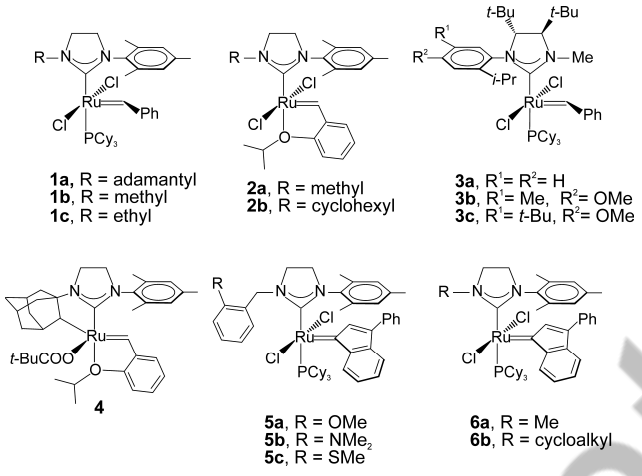

Chart 1. Selected catalysts with *N*-alkyl/*N*-aryl substituted NHCs

In this context, we recently[12] reported on new olefin metathesis catalysts bearing uNHCs, that combine *N*-cyclohexyl, *N*-isopropylphenyl groups and phenyl substituents on the NHC backbone with *syn* and *anti* relative orientation (**7**-**10**, Chart 2), thus investigating for the first time the impact of changing backbone configuration of uNHCs on catalytic behavior. As observed for Ru complexes bearing *syn* and *anti* backbone-substituted symmetrical NHCs,[8h,13] the introduction of differently oriented substituents on the backbone of uNHCs proved to be an effective means to modulate the catalytic properties of the resulting complexes.

To offer a more complete picture on the relationship between NHC architecture and catalyst activity, herein we present an extended study on the catalytic behavior of **7**-**10** in the most common metathesis transformations. The catalytic performances of **7**-**10** are compared to those of newly synthesized catalysts **11**-**14** (Chart 2), characterized by an *N*-alkyl group of reduced steric hindrance with respect to the *N*-cyclohexyl, as the *N*-methyl group.

Dalton Trans., 2016, 45, 561–571. doi: 10.1039/c5dt03758a

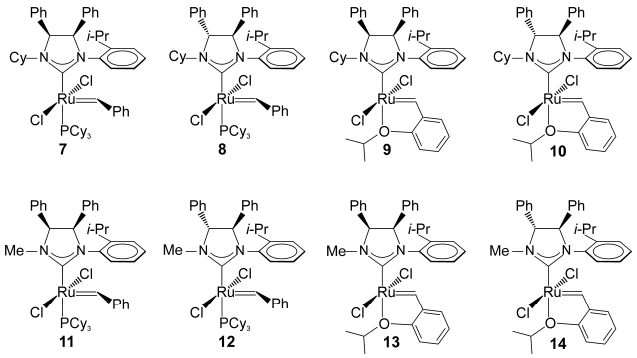

Chart 2. New *N*-alkyl/*N*-aryl NHC Ru catalysts

Furthermore, we report on the selectivity of enantiopure Ru catalysts **8**, **10**, **12** and **14** in asymmetric metathesis transformations, such as asymmetric ring-closing metathesis (ARCM) and asymmetric ring-opening cross-metathesis (AROCM).

Finally, in order to gain more insight into the role of NHC backbone configuration on catalytic behavior, the steric and electronic properties of uNHCs featuring catalysts **7**-**10** are evaluated using the corresponding rhodium complexes.

Results and discussion

Synthesis and characterization of Catalysts

The synthesis of complexes **7**-**10** was easily accomplished in three synthetic steps, as described in our preliminary communication.[12] The Grubbs' (**7**-**8**) and Hoveyda-Grubbs' (**9**-**10**) second generation type complexes were obtained in moderate to good yields (45-64%). All the complexes were found stable in the solid state for 5-6 months and in C_6D_6 solution over two weeks.[14] Solution-state 1D and 2D NMR analyses of the phosphine-containing complexes **7** and **8** showed the presence of two rotational isomers, *syn* and *anti*, corresponding to different orientations of the benzylidene unit with respect to the *N*-substituents of the uNHC ligand (*syn*: *N*-alkyl group located on the same side as the benzylidene unit).[15] These rotamers did not display chemical exchange on

Dalton Trans., 2016, 45, 561–571. doi: 10.1039/c5dt03758a

the NMR timescale up to 70°C, as proven by VT ^{1}H NMR experiments. Attempts to get good-quality crystals of **7** and **8** for X-ray crystallographic studies were unsuccessful.

As for phosphine-free complexes **9** and **10**, the formation of rotamers with only *anti* arrangement of the benzylidene moiety was observed in solution as well as in the solid state. The corresponding X-ray crystal structures have been previously reported.[12]

Complexes **11**-**14** were synthesized according to the synthetic route reported by Collins (Scheme 1).[16a,b] Starting from the commercial diamines **15** and **16**, cross-coupling with *o*-isopropylbromobenzene, followed by alkylation and cyclization in the presence of paraformaldehyde, afforded the aminals **19** and **20** in good yields (65 and 71%, respectively). After oxidation of **19** and **20** by treatment with I_2 and $NaHCO_3$ and anion exchange with $NaBF_4$, the corresponding tetrafluoroborate salts **21** and **22** were obtained in 66% and 78% yields, respectively. The deprotonation in situ of **21** and **22** with $(CF_3)_2(CH_3)COK$ and subsequent reaction with $RuCl_2(=CHPh)(PCy_3)_2$ (**GI**) or $RuCl_2(=CH\text{-}o\text{-}i\text{PrO-Ph})(PCy_3)$ (**HGI**) afforded, respectively, after flash column chromatography, the desired Grubbs' II (**11**-**12**) and Hoveyda-Grubbs' II (**13**-**14**) type complexes as air- and moisture-stable solids, albeit in very modest yields (12-22%). Attempts to improve yield by changing reaction conditions (e.g. nature of base, solvent and temperature) revealed unfruitful. The replacement of a large-sized cyclohexyl group with a sterically unencumbered methyl group led to a diminished stability of **11**-**14** with respect to **7**-**10**,[17] as proven by the disappearance from the ^{1}H NMR spectrum of the diagnostic benzylidene signal over the course of 1 week. This may also explain the differences in yield between **11**-**14** and **7**-**10**.

The solution-state studies carried out using 1D and 2D NMR techniques showed the presence of two rotational isomers for both **11** and **12**. As already observed for complexes **7** and **8**, the two rotamers are compatible with *syn* and *anti* disposal of the benzylidene moiety with respect to the *N*-substituents of the uNHC. Complex **11** was isolated in a 0.4:1 *syn*:*anti* ratio, while complex **12** in a ratio of 0.5:1 *syn*:*anti* isomers. 2D-EXSY experiments at various mixing times showed no exchange

Dalton Trans., 2016, 45, 561–571. doi: 10.1039/c5dt03758a

between *syn* and *anti* rotamers. Complexes **13**[18] and **14** were obtained as a single isomer, corresponding to the *anti* rotamer, analogously to what observed for **9** and **10**.[12] Unfortunately, owing to their high solubility in most common polar and non-polar solvents, it was no possible to obtain crystals suitable for X-ray solid-state characterization.

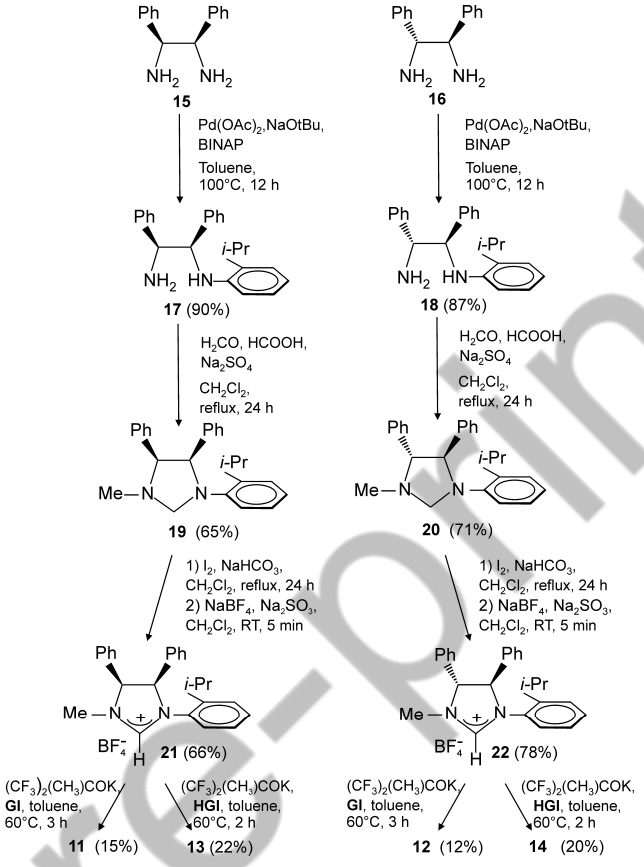

Scheme 1. Synthesis of new ruthenium complexes **11-14**

Ring-Closing Metathesis (RCM) Activity

The catalytic ability of **7-14** was investigated in the RCM reactions of diethyl diallylmalonate (**23**) and diallyltosylamine (**24**)**.** The RCM reactions promoted by Grubbs' II type complexes (**7**, **8**, **11** and **12**) were performed at 30°C in CD_2Cl_2, while the same ring-closures in the presence of Hoveyda-Grubbs' II type complexes (**9**, **10**, **13** and **14**) were carried out at 60°C in C_6D_6. Indeed, the latter family of ruthenium catalysts generally shows slow initiation rates under the catalytic

Dalton Trans., 2016, 45, 561–571. doi: 10.1039/c5dt03758a

conditions employed for the corresponding family of monophosphine complexes, therefore we selected reactions conditions more suitable to promote their activation.[13b]

The conversion of each substrate to product was monitored by ^{1}H NMR spectroscopy. To put the results in a larger context, we carried out parallel reactions with the symmetrical commercial catalysts **GII-tol**[19] and **HGII-tol**,[20] possessing low hindered *N*-aryl groups, as the catalysts **7**-**14**.

The kinetic profiles of all these experiments are depicted in Figure 1.

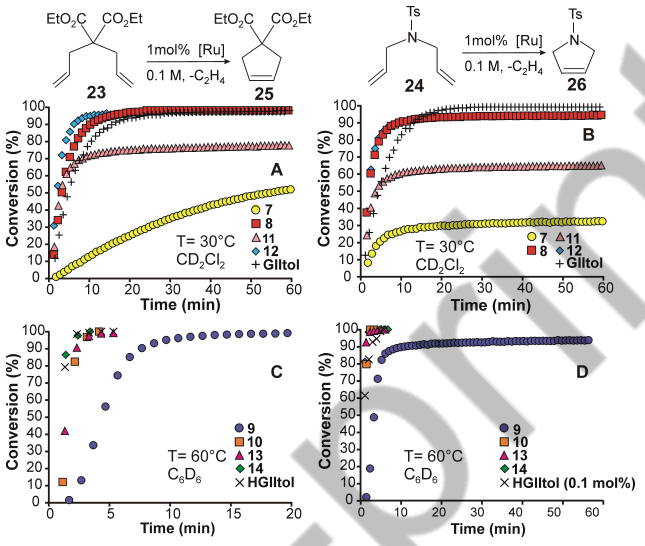

Figure 1. RCM conversion of **23** (A,C) and **24** (B, D)

Interestingly, a different catalytic behavior among ruthenium complexes with different NHC backbone configuration was observed. The phosphine-containing catalysts **8** and **12** with *anti* disposal of phenyl groups on the backbone showed very similar activities in both the RCM, overcoming significantly catalysts **7** and **11** with a *syn*-substituted backbone, and displaying faster initial reaction rates than the benchmark catalyst **GIItol**. Indeed, as emerges from the kinetic data of Figure 1A, **8** and **12** efficiently converted **23** to cyclic product **25** (>97% conversion) in 20 and 22 min, respectively, whereas **GIItol** needed 35 min to reach the same value of conversion. As for the RCM of tosylamine derivative **24** (Figure 1B), despite their higher initial reaction rates, **8** and **12** showed a slightly inferior efficiency (94% conversion in 35 min for both catalysts) with respect to **GIItol**, which effected complete cyclization (>99% conversion) in 27 min.

Dalton Trans., 2016, 45, 561–571. doi: 10.1039/c5dt03758a

Moreover, while for *anti* catalysts the size of the *N*-alkyl group (methyl or cyclohexyl) seems not to play a substantial role in the examined ring-closures, for *syn* catalysts it assumes appreciable relevance (Figure 1A, B). In fact, catalyst **11** bearing the smaller *N*-alkyl group performed much better than **7** with the more encumbered *N*-cyclohexyl group, furnishing the cyclic products **25** and **26** in 78% and 65 % conversion within 60 min, respectively. On the contrary, in the same time **11** effected the ring-closures of **23** and **24** in 52% and 32% conversion, respectively.

Quite surprisingly, as a general trend shown by **7**, **8**, **11** and **12**, and more markedly for *syn* catalysts, the RCM reactions of malonate derivative **23** revealed easier than those involving tosyl derivative **24**. This finding is uncommon, since *N*-tosyl derivatives are generally ring-closed with less difficulty with respect to malonate derivatives.[21] A clear evidence of this anomaly can be immediately caught by observing the kinetic profiles of the RCM of **23** and **24** promoted by **GIItol,** which indeed show a trend opposite to that of **7**-**11**.

As for phosphine-free complexes, reactivity differences in the RCM of **23** among **10**, **13**, **14** and **HGIItol** appeared to even out, very likely as a consequence of the higher temperature used to promote the activation of this class of catalysts (Figure 1C). Full conversions were reached in a range of 3-5 min, with *anti* catalysts **10** and **14** performing slightly better than *syn* catalyst with *N*-methyl group **13**, and rivaling with the benchmark catalyst **HGIItol**. A much minor efficiency was shown by *syn* catalyst **9**, bearing an *N*-cyclohexyl group, that produced the cycloolefin **25** in full conversion (>99%) within 20 min.

When the RCM of the *N*-tosylamine **24** was investigated, the same reactivity trend as that observed in the previous RCM was observed (Figure 1D). Catalysts **10**, **13** and **14** were able to complete cyclization in a range of 2-4 min, displaying a catalytic behavior comparable to that of **HGIItol** (full conversion in 6 min) at a ten times lower catalyst loading (0.1 mol%).[22] Also in this case, **9** revealed as the less efficient catalyst, not completing the RCM of **24** within 60 min (93% conversion). As already observed for the monophosphine complexes possessing equal NHC

Dalton Trans., 2016, 45, 561–571. doi: 10.1039/c5dt03758a

backbone configuration, the effect of the different bulkiness of the *N*-alkyl group is noticeable only for *syn* substituted catalysts.

The comparison on the catalytic behavior of catalysts **7**-**14** was then extended to the RCM of more hindered dienes **27** and **28**. The results for these reactions and for those promoted by **GIItol** and **HGIItol** are depicted in Figure 2. Again, phosphine-containing *anti* catalysts **8** and **12** gave better performances than their *syn* congeners (Figure 2A, B), with *anti* **8**, characterized by the bulkier *N*-cyclohexyl group, displaying the highest activity. Moreover, they were found more efficient than **GII tol** in both transformations. As previously observed, the hindrance of the *N*-alkyl substituent strongly influences the reactivity of *syn* catalysts; however, in the latter case, the catalytic performances of complexes **7** and **11** were inverted, and the presence of the more encumbered *N*-alkyl group (*N*-Cy) resulted in better catalytic activity. A careful analysis of the slope of the corresponding curves in Figure 2A and 2B strongly suggests a higher decomposition rate of **11** with respect to **12**, reflecting very likely the different stability associated to each of them. It is worth to note that the reactivities of **7**-**12** towards malonate derivative **27** were slightly lower than those towards tosyl derivative **28**, differently from what observed for the RCM of the less sterically encumbered diolefins **23** and **24**.

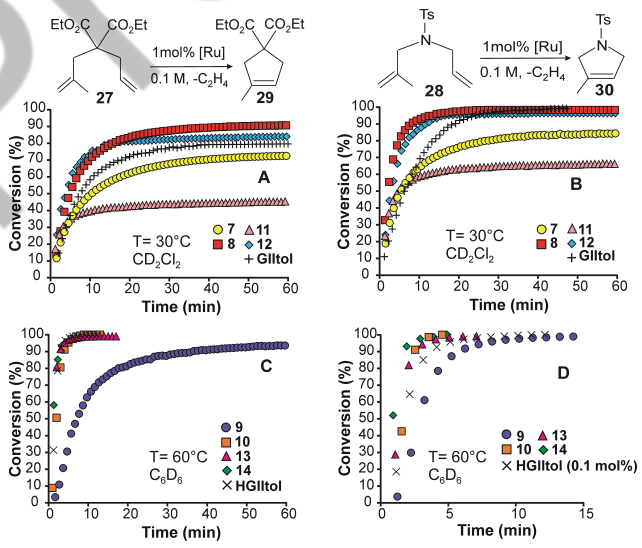

Figure 2. RCM conversion of **27** (A,C) and **28** (B, D)

Dalton Trans., 2016, 45, 561–571. doi: 10.1039/c5dt03758a

The kinetic plots for the RCM of **27** and **28** promoted by phosphine-free catalysts **9**, **10**, **13**, and **14** are sketched in Figure 2C and 2D, respectively. The general reactivity trend is in line with that previously observed for the RCM reactions carried out with this family of complexes, with very little marked. differences in the catalytic behavior. *Anti* catalysts **10** and **14** were able to quantitatively convert **27** to cycloolefin **29** within 9 min, as well as the commercial available **HGIItol**, proving to be somewhat more efficient than *syn* **13,** which instead required 12 min to reach full conversion. Again, *syn* **9** revealed as the less efficient catalyst, nearly completing the same reaction (94% conversion) within 60 min (Figure 2C) . Differences among the tested catalysts in overall activity were more evident in the ring-closure of **28**. *Anti* catalysts needed 5 min to give quantitative conversion to cyclic product **30**, outperforming **HGIItol** (>99% in 12 min) and *syn* catalysts **9** and **13**. Between the latter two catalysts, *syn* **13** with less hindered *N*-methyl group furnished **30** in complete conversion within 7 min, whereas **9** took twice as long (Figure 2D). These experimental evidences are in contrast with the results obtained with the corresponding monophosphine catalysts, where the *syn* catalyst with *N*-methyl group revealed minor efficiency than the *syn* catalyst with *N*-cyclohexyl group. Very likely, the increased stability, typical of phosphine-free catalysts, strongly influences the reactivity trend.

We also investigated the catalytic properties of **7**-**14** in the challenging RCM of sterically encumbered dienes **31** and **32**. The corresponding kinetic data, depicted in Figure 3, disclosed a striking reactivity difference among *anti* catalysts **8** and **10**, with the bulkier *N*-cyclohexyl group, and all the other ones. In the RCM of **31** (Figure 3A), *anti* **8** furnished the cyclic product **33** with a 57% conversion, inferior only to the benchmark catalyst **GIItol**, which is particularly competent in difficult RCM reactions. A lower conversion was registered with phosphine-containing *anti* catalyst **12**, possessing the less bulky *N*-methyl group, which slightly surpassed *syn* **9** with *N*-cyclohexyl group to provide **33** (30% vs 22% conversion). The worst RCM performance was given by *syn* catalyst **11**, which achieves only 9% conversion within 60 min. A very similar catalytic behavior

Dalton Trans., 2016, 45, 561–571. doi: 10.1039/c5dt03758a

was noticed in the RCM of tosyl derivative **32** (Figure 3B), where *anti* **8**, once again, turned out to be the most active among the newly synthesized catalysts (64% conversion within 60 min), while differences among **7**, **11** and **12** are nearly undetectable (around 30% conversion). As in the RCM of malonate derivative **31**, **GIItol** disclosed the highest propensity to the ring closure of **32** (92% conversion in 60 min).

As depicted in Figure 3C, the phosphine-free catalyst **10**, successfully accomplished the ring-closing of **31** (>97 conversion), equaling the performance of the commercial benchmark **HGIItol**, which is one of the most efficient catalyst in RCM reactions of encumbered substrates.[6b]

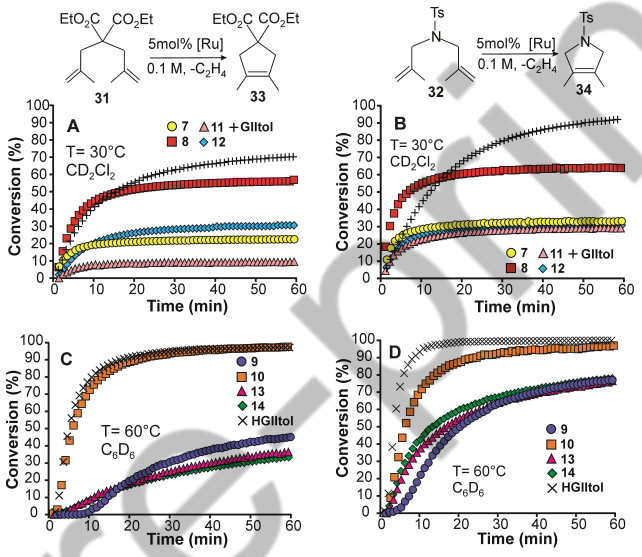

Figure 3. RCM conversion of **31** (A,C) and **32** (B, D)

Moreover, it significantly outperformed **9**, **13** and **14**, which indeed, in the same time, achieved conversions in a range of 33-45%. In the RCM of **32** (Figure 3D), **10** behave as in the previous RCM (97% conversion within 60 min), exhibiting inferior catalytic performance with respect to **HGIItol**, which reached a 99% conversion in 20 min. Catalysts **9**, **13** and **14** gave each one the same value of conversion (77%), displaying slightly better efficiency than in the RCM of malonate derivative **31.**

The above results suggest that catalysts with an *anti* disposal of the phenyl groups on the NHC backbone are more active than their *syn* analogues, and that the size of the *N*-alkyl groups (methyl

Dalton Trans., 2016, 45, 561–571. doi: 10.1039/c5dt03758a

or cyclohexyl) plays an important role in determining catalytic behavior. Indeed, *anti* catalysts benefit from the steric hindrance offered by the *N*-cyclohexyl group in exhibiting superior catalytic performances in almost all cases, especially in the RCM of **31** and **32** leading to tetrasubstituted olefins. On the contrary, the bulkier *N*-cyclohexyl seems to be responsible for the mediocre RCM performances of *syn* catalysts, which disclosed an unexpectedly low activity in the easier RCM reactions. To rationalize the peculiar behavior of *syn* catalysts toward low hindered olefins as **23**, we reasoned on the possibility that RCM nonproductive events could play an important role in influencing the outcome of the reaction.[23] Therefore, to probe this hypothesis, molecular modeling studies were carried out (see Supporting Information for computational details).

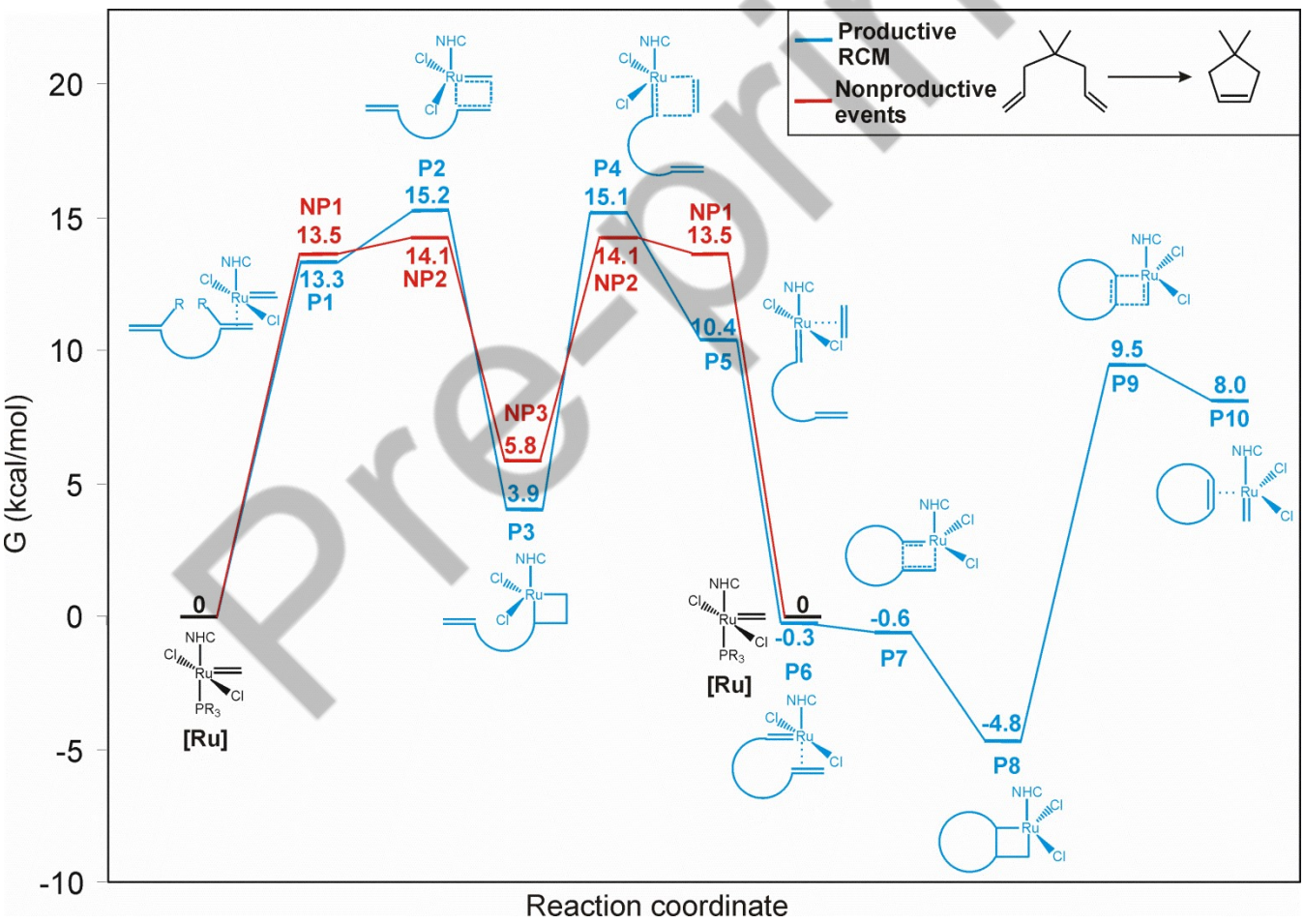

Figure 4. Free energy profile in CH_2Cl_2 solution of the RCM of a model of **23** promoted by catalyst **7**, compared to nonproductive event energy profile.

Dalton Trans., 2016, 45, 561–571. doi: 10.1039/c5dt03758a

The free-energy profile for the RCM of a model of **23** (in which the -COOEt group has been replaced by a -CH_3) with catalyst **7** was compared with nonproductive event energy profile. As depicted in Figure 4, rate determining transition state for the RCM was found to be the first cross metathesis between the substrate and the alkylidene species (P2 in Figure 5), as already reported for analogous catalytic systems.[13b,24] More in detail, minimum energy profile involves species characterized by alkylidene oriented under the aryl moiety, while higher energy transition states were located when the alkylidene is under the cyclohexyl group. $\Delta G^{\neq}$ of P2 was calculated to be 15.2 kcal/mol in CH_2Cl_2, being significantly higher than barriers found for **23** for analogous systems symmetrically substituted on nitrogen atoms.[13b]

On the contrary, transition state for nonproductive events (NP2 in Figure 5) presents lower free energy, being favored of 1,1 kcal/mol (in CH_2Cl_2) with respect to P2, with an absolute barrier of 14,1 kcal/mol. Based on DFT calculation results, the extraordinary low activity of catalyst **7** in the RCM of low hindered substrates seems to be depending on the high frequency of nonproductive events, that appear to be favored with respect to productive catalytic cycle. This hypothesis is also corroborated by previous experimental studies, that showed the increasing of nonproductive events in the presence of unsymmetrical NHCs with respect to symmetrical ones.[23]

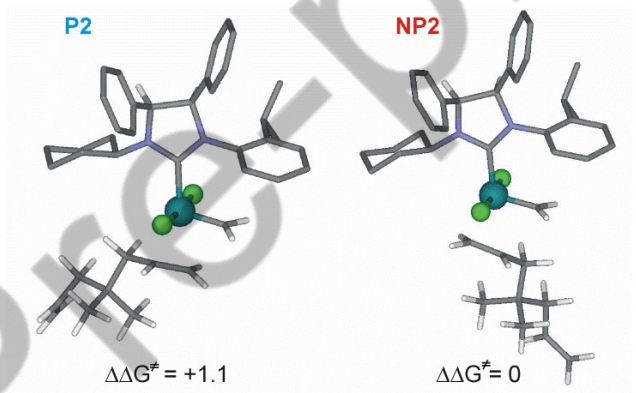

Figure 5. Structures of rate determining step transition state of RCM of **23** (P2) and of nonproductive event transition state (NP2)

Ring-Opening Metathesis Polymerization (ROMP) activity

To further assess the reactivity of **7**-**14**, we turned out our attention to the ROMP of 1,5-cyclooctadiene (**35**). This reaction was monitored by ^{1}H NMR (Figure 6), and the results are summarized in Table 1. All the four catalysts were found efficient, with the *anti* isomers again outperforming the corresponding *syn* isomers. In particular, monophosphine catalysts **8** and **12**, with

anti phenyl groups on the NHC backbone, quantitatively furnished poly(**35**) in 20 and 9 minutes, respectively, displaying activities lower than that of the reference catalyst **GIItol** (Figure 6A; entry 5, Table 1). Instead analogous *syn* isomers **7** and **11** required 30 and 14 min, respectively, to successfully accomplish the polymerization. Furthermore, the smaller is the *N*-alkyl group, the higher is the catalytic activity (entries 1-4, Table 1). Very likely, the presence of a less bulky methyl group facilitates the approach of **35** to the ruthenium centre.

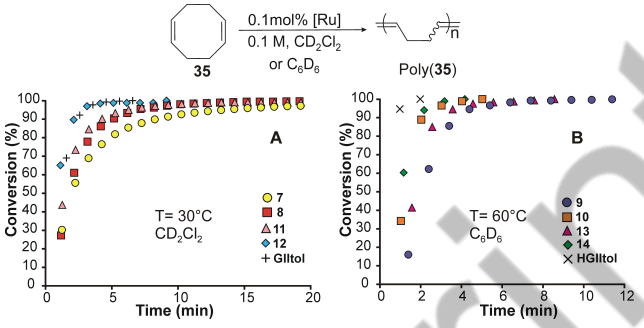

Figure 6. ROMP conversion of **35**.

The same reactivity trend was observed with phosphine-free catalysts **9**-**14** (Figure 6B), even if reactivity differences appeared to be levelled out. All the catalysts exhibited lower efficiency than the benchmark catalyst **HGIItol** (entries 6-10, Table 1). As for *E:Z* selectivity, catalysts **7**-**14** disclosed *E:Z* ratios inferior to those of **GIItol** and **HGIItol**, and a certain degree of *Z* selectivity could be appreciated in the ROMP reactions carried out with catalysts bearing the less encumbered *N*-methyl group (entries 3, 4, 8 and 9, Table 1). It is reasonable to suppose that the high level of dissymmetry, created by substituents on the nitrogen atoms with such a different steric hindrance, may influence the selectivity of key metathesis intermediates.[10b,d]

Dalton Trans., 2016, 45, 561–571. doi: 10.1039/c5dt03758a

Table 1. ROMP of **35**

entry	catalyst	time (min)	poly(**35**) yield[a] (%)	E:Z[b]
1[c]	7	30	98	1.0
2[c]	8	20	>99	1.0
3[c]	11	14	99	0.8
4[c]	12	9	>99	0.5
5[c]	GIItol	4	>99	1.3
6[d]	9	12	>99	2.0
7[d]	10	5	>99	2.5
8[d]	13	8	>99	0.9
9[d]	14	4	>99	2.0
10[d]	HGIItol	2	>99	3.8

[a]Determined by ^{1}H NMR. [b]E/Z ratios were determined by ^{1}H and ^{13}C NMR of isolated products. [c]Reactions in CH_2Cl_2, at 30°C, catalyst 0.1 mol%. [d]Reactions in C_6D_6, at 60°C, catalyst 0.1 mol%.

Cross-Metathesis (CM) activity

Afterward, the catalytic behavior of **7**-**10**[12] was compared to that of newly synthesized **11**-**14** in the CM of allyl benzene (**36**) and *cis*-1,4-diacetoxy-2-butene (**37**). The reaction is illustrated in Scheme 2 and the results are reported in Table 2.

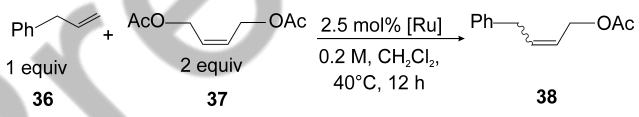

Scheme 2. CM of substrates **36** and **37**

In contrast with the above experimental data, in this metathesis reaction catalysts with *syn* oriented phenyl groups on the NHC backbone were found to be more competent than their *anti* congeners, affording high yields combined to low *E/Z* ratios (~ 3) in the presence of catalysts **7** and **9**, possessing an encumbered *N*-cyclohexyl group (entries 1 and 6, Table 2). Indeed, catalysts with the smaller *N*-methyl group gave worse results, in terms of both conversion in the desired product and *E/Z* selectivity (entries 3 and 8, Table 2), resembling those of classical symmetrical second generation catalysts.[25]

Dalton Trans., 2016, 45, 561–571. doi: 10.1039/c5dt03758a

Table 2. CM of **36** and **37** promotes by catalysts **7-14**

entry	catalyst	**38** yield[a] (%)	E:Z[b]
1	7	88	3.6
2	8	53	8.5
3	11	66	7.4
4	12	53	9.5
6	9	72	2.6
7	10	67	7.6
8	13	86	8.0
9	14	57	8.6
1	7	88	3.6
2	8	53	8.5

[a]Isolated yield. [b]*E:Z* ratios were determined by ^{1}H NMR spectroscopy.

It is worth to note that yields in the desired cross-coupling product **38** are always higher for *syn* catalysts with respect to the *anti* analogues, although conversions of **36** are almost quantitative (> 90%). This suggests a major tendency of *anti* catalysts to give the homocoupling product of **36** (1,4-diphenyl-2-butene) rather than **38**.

The above results point out that uNHC backbone configuration could cause profound alteration of the shape of the reactive pocket around the metal, thus addressing not only activity but also selectivity of the corresponding Ru complexes. Moreover, since marked differences in selectivity between *anti* and *syn* catalysts were registered only in the presence of the more encumbered *N*-cyclohexyl group, a combined effect of backbone configuration and bulkiness of *N*-substituents is unquestionable.

It is important to underline that we are not able to evaluate the effect that each rotational isomer (*syn* and *anti*) of complexes **7-12** exerts on catalyst properties due to the fact that the *syn:anti* isomers can not be separated. However, the strong similitude of behavior between monophosphine and phosphine-free catalysts (obtained as *anti* rotational isomers only) in both RCM and CM

Dalton Trans., 2016, 45, 561–571. doi: 10.1039/c5dt03758a

reactions strongly suggest the primary role of the backbone configuration in influencing catalyst behavior with respect to the existence of rotamers.

Asymmetric metathesis transformations

Finally, the enantiopure catalysts **8**, **10**, **12**, and **14** were evaluated in some model asymmetrical metathesis reaction, such as asymmetric ring-closing metahesis (ARCM) of achiral trienes **39** and **40** (Scheme 3) and asymmetric ring-opening cross-metahesis (AROCM) of the *meso*-norbornene **43** and styrene (Scheme 4).

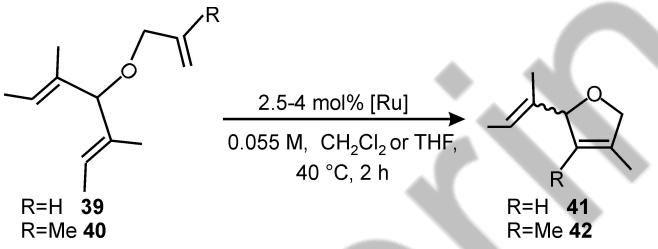

Scheme 3. ARCM of **39** and **40**

The results for the ARCM of trienes **39** and **40** are summarized in Table 3. All the catalysts were able to promote the ring closure of **39** in high yields. The enantiomeric excesses were modest (18-33%, entries 1, 3, 5 and 7, Table 3); however, in analogy with what observed in ARCM reactions with chiral catalysts bearing C_2-symmetric NHCs,[26] they were increased by employing NaI as an additive (47-53% ee) (entries 2, 4, 6 and 8, Table 3). This finding is in contrast with the study by Collins on the same ARCM reaction performed with chiral catalysts incorporating C_1-symmetric NHCs, structurally very similar to the ones newly synthesized. Indeed, in that case, a deleterious impact of the use of NaI on enantioselectivity was observed (entries 9 and 10).[16a,b]

As a further remark, by comparison the results for the ring closure of **39** carried out with catalysts **12** and **3a**, which differ only for the steric hindrance of substituents on the NHC backbone (phenyl vs t-butyl groups), a great difference in enantioselectivity emerged. A nearly negligible effect of the

Dalton Trans., 2016, 45, 561–571. doi: 10.1039/c5dt03758a

size of *N*-substituents on enantiomeric excesses was detected (entries 1 and 3, Table 3), and no substantial variations in yields and in enantioselectivies were noticed moving from phosphine-containing to phosphine-free catalysts (entries 1-4 and 5-8). This suggests that enantioenrichment of **41** is determined by the same catalytic intermediate, independently of the fact that phosphine-containing catalysts are a mixture of rotamers, while phosphine-free catalysts consist of a single rotational isomer.

The good performances exhibited by catalysts **8**, **10**, **12**, and **14** in the ring-closing of hindered substrates prompted us to investigate their behavior in the challenging ARCM of **40** to generate tetrasubstituted olefin **42.** All the catalysts were found to be competent in this sterically demanding reaction, disclosing opposite enantioselectivity with different values depending on the *N*-alkyl substituents. Catalysts **8** and **10**, characterized by an *N*-cyclohexyl group, furnished almost quantitatively the cyclic product **42** (>95% conversion, 42% ee, entries 11 and 15, Table 3), outperforming catalyst **3** (95% conversion, 8% ee, entry 19, Table 3) and mirroring the best results reported by Collins with modified versions of catalyst **3** (95% conversion, 43% ee).[16c]

On the other hand, catalysts **12** and **14** successfully accomplished the RCM of **40** (>98% conversion) in 25% and 29% ee of the opposite enantiomer, respectively. This clearly indicates that the *N*-alkyl group of the NHC ligand has a direct effect on the enantiomeric excesses of the desymmetrization reaction. Also in this case, by changing substituents on the NHC backbone (as from **3** to **12**), catalyst properties changed (compare entry 10 to entries 13 and 17 of Table 3). The addition of NaI to improve enantioselectivity completely shut down the reaction, very likely because the replacement of Cl^- bound to ruthenium with I^- ligands makes too congested the reactive pocket of the catalyst, thus rendering difficult the approach of the bulky substrate **40**. As observed in the RCM of **39**, Grubbs' II and Hoveyda-Grubbs II type catalysts showed the same catalytic behavior.

Dalton Trans., 2016, 45, 561–571. doi: 10.1039/c5dt03758a

Further studies to identify *N*-alkyl groups more suitable to increase enantiomeric excesses in desymmetrization reaction of *meso*-trienes and to shed light on the involved mechanism of enantioinduction are underway.

Table 3. ARCM of **39** and **40** with **8**, **10**, **12** and **14**

entry[a]	substrate	catalyst (mol%)	Additive	Yield[b] (%)	ee[c] (%)
1[d]	39	**8** (2.5)	none	>98	18 (*S*)
2[d]	39	**8** (4.0)	NaI	>95	53 (*S*)
3	39	**12** (2.5)	none	>98	33 (*S*)
4	39	**12** (4.0)	NaI	>98	50 (*S*)
5[d]	39	**10** (2.5)	none	>98	19 (*S*)
6[d]	39	**10** (4.0)	NaI	>95	52 (*S*)
7	39	**14** (2.5)	none	>98	33 (*S*)
8	39	**14** (4.0)	NaI	>98	47 (*S*)
9[e]	39	**3a** (2.5)	none	>95	82 *(S)*
10[e]	39	**3a** (4.0)	NaI	>95	48 *(S)*
11[f]	40	**8** (2.5)	none	>95	42 *(S)*
12[f]	40	**8** (4.0)	NaI	-	-
13	40	**12** (2.5)	none	>98	25 (*R*)
14	40	**12** (4.0)	NaI	-	-
15[f]	40	**10** (2.5)	none	>95	42 (*S*)
16[f]	40	**10** (4.0)	NaI	-	-
17	40	**14** (2.5)	none	>98	29 (*R*)
18	40	**14** (4.0)	NaI	-	-
19[g]	40	**3a** (2.5)	none	95	8 (S)

[a]Runs without additive were carried out in CH_2Cl_2, while runs with NaI were performed in THF. [b] Yields based on NMR analysis. [c]Enantiomeric excesses determined by chiral GC. [d]Taken by ref. 12. [e]Ref.16a,b. [f]Taken by ref. 12. [g]Ref.16c.

Our attention was then focused on AROCM, that represents a powerful method for the construction of enantioenriched dienes, employed as the key step in several total syntheses.[27] Table 4 described

Dalton Trans., 2016, 45, 561–571. doi: 10.1039/c5dt03758a

the results for the AROCM of *cis*-5-norbornene-*endo*-2,3-dicarboxylic anhydride (**43**) with styrene as the model reaction (Scheme 4).

The *meso*-norbornene **43** was reacted with 10 equivalents of styrene in the presence of monophosphine catalysts **8** and **12** and of phosphine-free catalysts **10** and **14** at room temperature, for 2 and 4 hours, respectively. The reactions promoted by the more encumbered catalysts **8** and **10** gave **44** in moderate enantioselectivity (29-32% ee, entries 1 and 3, Table 4). Employment of catalysts **12** and **14**, with reduced steric hindrance, resulted in lower enantiomeric excesses (10-13%, entries 2 and 4, Table 4). Except stilbene arising from the cross-metathesis of styrene, no polymer or homometathesis product was detected in the reaction mixture. All the products showed *trans* stereochemistry, and no *cis* isomers were observed.

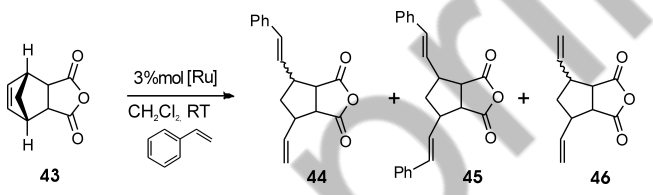

Scheme 4. AROCM of **43** and side-products

As reported by Grubbs for the analogous AROCM transformation promoted by chiral *N*-aryl, *N*-alkyl NHC ruthenium catalysts,[28] the formation of AROCM side products **45** and **46** was observed. Grubbs' II- type catalysts and the corresponding Hoveyda-Grubbs' II- type catalysts provided slightly different ratios of products **44**, **45** and **46**.

Further investigations to elucidate the pathway to the formation of these two side products, in order to better assess catalytic properties of this class of chiral unsymmetrical NHC ruthenium complexes, are ongoing.

Dalton Trans., 2016, 45, 561–571. doi: 10.1039/c5dt03758a

Table 4. AROCM of **43** with styrene

entry[a]	cat.	**44** yield[b] (%)	**45** yield[b] (%)	**46** yield[b] (%)	ee (**44**)[c] (%)
1[d]	**8**	45	10	10	32
2[e]	**10**	46	15	10	13
3[d]	**12**	20	5	11	29
4[e]	**14**	35	7	24	10

[a][**43**]: 0.07 M in CH_2Cl_2; 10 eq. styrene. [b]Isolated yield. [c]Enantiomeric excess determined by chiral HPLC. [d]Reaction time: 2h. [e]Reaction time: 4h

Steric and electronic properties of uNHCs

The comparison among catalytic behaviors of ruthenium complexes, with different NHC backbone configuration and different *N*-alkyl substituents, highlighted major reactivity differences mainly between *syn* and *anti* complexes characterized by the more encumbered *N*-cyclohexyl group. Intrigued by this experimental evidence, we decided to gain more insight into the steric and electronic properties of these latter uNHCs using the corresponding rhodium complexes. New rhodium cyclooctadiene complexes (**47**, **48)** and bis(carbonyl)complexes (**49**, **50**) were prepared with previously described procedures.[8d] (Scheme 5).

Deprotonation of dihydroimidazolium salts **A** and **B** with potassium hexamethyldisilazide (KHMDS) in toluene at room temperature, and subsequent treatment with $[RhCl(COD)]_2$ afforded, after purification by column chromatography, **47** and **48** in 84% and 79% yield, respectively (Scheme 5). The desired products were isolated as yellow microcrystalline solids.

^1H and ^{13}C NMR spectroscopic analyses of complexes **47**, characterized by a *syn* disposal of phenyl groups on the NHC backbone, revealed the presence of two isomers (molar ratio 1:0.2), due to a restricted rotation around the Rh-NHC bond or around the N-aryl bond.[29]

Dalton Trans., 2016, 45, 561–571. doi: 10.1039/c5dt03758a

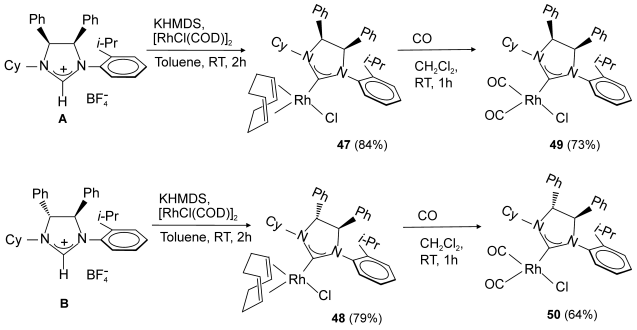

Scheme 5. Synthesis of Rh complexes **47**-**50**

^{1}H and ^{13}C NMR spectroscopic analyses of complexes **47**, characterized by a *syn* disposal of phenyl groups on the NHC backbone, revealed the presence of two isomers (molar ratio 1:0.2), due to a restricted rotation around the Rh-NHC bond or around the N-aryl bond. Only one rotamer was indeed observed for complex **48**, with *anti* phenyl groups on the backbone. The signals due to the carbenic carbon coordinated to the metal were observed at 216.9 ppm (major isomer, d, $J_{Rh\text{-}C}$ = 48.1 Hz) and 214.9 ppm (d, $J_{Rh\text{-}C}$ = 47.2 Hz) for the complexes **47** and **48**, respectively.

Single crystals suitable for X-ray structure analysis were obtained for both complexes by slow evaporation of concentrated solutions in CH_2Cl_2 . The crystal structures are shown in Figure 6, and selected bond lengths and angles can be found in Table 5. In both compounds, the Rh center adopts a square planar coordination geometry. The chlorine atoms and the C1(NHC) atoms are *trans* oriented to the C=C π systems of the COD alkene molecule. Complex **47** crystallizes in the centrosymmetric space group *C2/c*, accordingly, the crystal contains a racemic mixture of both the enantiomers having opposite configurations of C2 and C3 carbon atoms (*RS* and *SR*) of NHC ligand. Conversely, complex **48** crystallizes in the orthorhombic non-centrosymmetric space group $P2_12_12_1$ where both the asymmetric C2 and C3 atoms exhibit *R* chirality. It was possible to determine the absolute configuration from the crystallographic data by means of the calculated Flack parameter of -0.02(5).[30]

Dalton Trans., 2016, 45, 561–571. doi: 10.1039/c5dt03758a

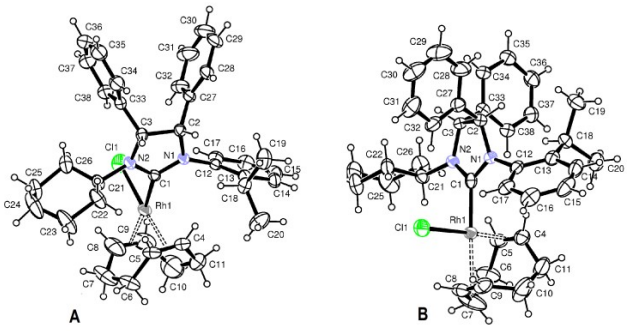

Figure 6. ORTEP[31] view of complexes **47** (A) and **48** (B) with the thermal ellipsoids at 30% probability.

In both complexes the distances of the Rh to the centroids of the COD alkene bonds are longer for those *trans* to NHC [2.099(4) Å for **47**, 2.102(8) Å for **48**] than for those *trans* to chlorine atom [1.974(4) Å for **47**, 1.975(8) Å for **48**]. This can be ascribed to the greater *trans* influence of the NHC moiety.

All the other structural parameters are in good agreement with those observed for other similar complexes.[32-35]

The steric bulk, measured as the percentage of buried volume (%V_{Bur}) of the *N*-cyclohexyl/*N*-*o*-isopropylphenyl NHC ligands with *syn* or *anti* phenyl groups on the backbone, was extracted using the Samb*V*ca program developed by Cavallo,[36] using the crystal data of the corresponding Rh complexes **47** and **48**. The %V_{Bur} values are 29.7 and 29.9 for *syn* uNHC and *anti* uNHC ligand, respectively, thus within the same level of significance.[37]

In order to study the electronic properties of these ligands, the *cis*-dicarbonyl complexes **49** and **50** were synthesized by replacing the COD ligand in **47** and **48** with carbon monoxide, as depicted in Scheme 5. The ^{1}H NMR spectra of **49** and **50** confirmed the disappearance of the signals due to the COD ligand. Complexes **49** and **50** were obtained as a mixture of two isomers (molar ratio 1:0.1 for **49**, 1: 0.3 for **50**), as a consequence of a restricted rotation around the Rh-NHC bond or around the

Dalton Trans., 2016, 45, 561–571. doi: 10.1039/c5dt03758a

N-Ar bond.[29] The ^{13}C NMR spectra showed the signals assigned to the carbene carbon at 206.3 ppm (major isomer, d, J_{Rh-C}=38.9Hz) for **49**, and at 203.2 ppm (d, J_{Rh-C}=40.4Hz) for **50**. The ^{13}C NMR chemical shifts of the two carbonyl ligands were observed for the major isomer of **49** at 186.8 (d, J_{Rh-C}=53.4Hz) and 183.5 ppm (d, J_{Rh-C}=75.5Hz), while for **50** at 186.7 (d, J_{Rh-C}=54.3Hz) and 183.7 ppm(d, J_{Rh-C}=73.9Hz).

Table 5. Selected bond distances and angles (Å and degrees).

Distances	**47**	**48**
Rh1-C1	2.016(2)	1.999(6)
Rh1-Cl1	2.3825(8)	2.388(2)
Rh1-***C***(C4-C5)*	1.974(4)	1.975(8)
Rh1-***C***(C8-C9)*	2.099(4)	2.102(8)
C1-N1	1.344(4)	1.358(8)
C1-N2	1.337(4)	1.347(7)
Angles		
C1-Rh1-Cl1	86.18(7)	90.0(2)
C1-Rh1-***C***(C4-C5)	95.0(1)	92.0(2)
C1-Rh1-***C***(C8-C9)	174.6(1)	177.8(2)
Cl1-Rh1-***C***(C4-C5)	176.8(1)	177.8(2)
Cl1-Rh1-***C***(C8-C9)	90.9(1)	91.0(2)
C(C4-C5)-Rh1- ***C***(C8-C9)	88.1(1)	87.0(2)
N1-C1-N2	109.0(2)	107.2(5)
C1-N1-C2	113.1(2)	112.9(5)
C1-N2-C3	113.6(2)	113.4(5)

* Centroids of the COD C4=C5 and C8=C9 double bonds.

The IR spectra of dicarbonyl complexes **49** and **50** were recorded in the solid-state (KBr) and carbonyl stretching frequencies were found to be significantly dependent on the NHC backbone configuration. More in detail, complex **49** with *syn* phenyl groups on the NHC backbone showed signals due to the stretching of the two CO ligands at 2080 and 1999 cm^{-1}, whereas the *anti* isomer **50** exhibited the analogous signals at 2075 and 1992 cm^{-1}. The Tolman electronic parameter (TEP) of the uNHCs coordinated to **49** and **50** was then estimated from the average stretching vibration

Dalton Trans., 2016, 45, 561–571. doi: 10.1039/c5dt03758a

wavenumber (2039.5 cm^{-1} for the uNHC from **49**, and 2033.5 cm^{-1} for the uNHC from **50**), by using the linear regression proposed by Droge and Glorius.[38] This led to a value of 2051.8 cm^{-1} for uNHC from **49** and of 2047.0 cm^{-1} for uNHC from **50**, suggesting a more electron-donating nature for the uNHC bearing *anti* phenyl groups on the backbone than for the one bearing *syn* oriented phenyl group.

Bond-dissociation energies (BDE) for uNHC ligand from Rh carbonyl complexes **49** and **50** were evaluated by DFT calculations (see Supporting information for computational details) and were found to be 55,86 kcal/mol for **49** and 56.44 kcal/mol for **50**. Therefore, dissociation of NHC ligand with *anti* phenyl groups on the backbone is more expensive of about 0.6 kcal/mol than dissociation of NHC with *syn* phenyl groups, corroborating the hypothesis that lower CO stretching frequencies are associated to higher NHC-Rh bond strength. This is also supported by the analysis of the NHC-Rh bond distances in the corresponding rhodium-COD complexes **47** and **48**, where the bond distance between the NHC carbene carbon and the Rh center is shorter in **48** (1.999 Å) than in **47** (2.016 Å).

In the light of these results, it can be reasonably assumed that electronic factors outweigh steric factors for uNHCs presenting different backbone configuration, and that this feature could be related to the different efficiency shown by the corresponding ruthenium complexes **7**-**10** in the examined olefin metathesis transformations.

Conclusion

In summary, we have presented herein the synthesis and characterization of four new Grubbs' and Hoveyda-Grubbs' second generation catalysts (**11**-**14**) bearing unsymmetrical NHC ligands with *N*-methyl/N-isopropylphenyl substituents and *syn* or *anti* phenyl groups on the backbone. The catalytic behavior of these complexes was evaluated in standard RCM, ROMP and CM reactions and compared to that of analogous complexes presenting a more encumbered *N*-cyclohexyl group

Dalton Trans., 2016, 45, 561–571. doi: 10.1039/c5dt03758a

(**7**-**10**). While *anti* substituted catalysts benefit of the steric hindrance offered by the *N*-cyclohexyl group, achieving the best catalytic efficiencies in almost all the metathesis transformations, and demonstrating to be particularly competent in the most challenging RCM reactions, for *syn* catalysts the presence of the bulkier *N*-cyclohexyl group is detrimental. In particular, catalysts **7** and **9** showed low activities in the easier RCM reactions, and this peculiar behavior, rationalized by DFT calculations, was ascribed to a major tendency of these catalysts to give nonproductive metathesis events. This feature strongly suggest to exploit these catalysts for targeted reactions, such as ethenolysis.

The enantiopure catalysts **8**, **10**, **12** and **14** were also compared in asymmetric metathesis transformations, showing moderate enantioselectivity in both ARCM and AROCM. A clear influence of the bulkiness of the *N*-alkyl groups on the enantiomeric excesses was observed, encouraging further efforts towards the design of new chiral catalysts by varying the size of *N*-alkyl substituents.

Finally, the steric and electronic properties of *N*-cyclohexyl/*N*-isopropylphenyl NHC ligands were evaluated from the corresponding rhodium cyclooctadiene (**47**, **48**), characterized by X-ray analysis, and rhodium dicarbonyl (**49**, **50**) derivatives. To the best of our knowledge, this represent the first example of rhodium complexes bearing backbone-substituted unsymmetrical NHCs. While the percentage of buried volume (%V_{Bur}) indicate very similar steric properties for the uNHCs with different backbone configuration, the Tolman electronic parameter revealed a more electron-donating character for uNHC with *anti* configuration, suggesting a direct correlation with the catalytic properties shown by the corresponding catalysts.

A deeper investigation on the impact of unsymmetrical NHC ligands differing for backbone configuration and *N*-alkyl/*N*-aryl substituents on catalyst properties are in progress.

Dalton Trans., 2016, 45, 561–571. doi: 10.1039/c5dt03758a

Acknowledgements

The authors thank Dr Patrizia Iannece, Dr Ivano Immediata, Patrizia Oliva for technical assistance and Dr Alessandra Perfetto for some experimental work. F.G. thanks prof. Luigi Cavallo for his valuable suggestions on using the web application Samb*V*ca. Financial support from the Ministero dell'Università e della Ricerca Scientifica e Tecnologica is gratefully acknowledged.

Notes

Electronic Supplementary Information (ESI) available: Experimental procedures, figures giving NMR spectra of the new complexes, GC and HPLC chromatograms of **39**, **40** and **44**, tables and CIF files giving experimental details for complexes **47** and **48**, and Cartesian coordinates for the optimized structures.

References

1 (*a*) H.-W. Wanzlick, H.-J. Schönherr, *Angew. Chem., Int. Ed.*, 1968, **7**, 141; (*b*) K. Öfele, *J. Organomet. Chem*., 1968, **12**, P42.

2 (*a*) *N-Heterocyclic Carbenes: Effective Tools for Organometallic Synthesis*; ed. S. P. Nolan, Wiley-VCH, 2014; (*b*) M. N. Hopkinson, C. Richter, M. Schedler, F. Glorius, *Nature*, 2014, **510**, 485; (*c*) *N-Heterocyclic Carbenes in Transition Metal Catalysis and Organocatalysis;* C. S. J. Cazin, Springer, 2011; (*d*) *N-Heterocyclic Carbenes in Synthesis;* ed. S. P. Nolan, Wiley-VCH, Weinheim, Germany, 2006; (*e*) *N-Heterocyclic Carbenes in Transition Metal catalysis*; ed. F. Glorius, Springer-Verlag, Berlin, Germany, 2007; (f) C. M. Crudden; D. P. Allen, *Coord. Chem. Rev.* 2004, **248**, 2247; (*g*) A. Correa, S. P. Nolan, L. Cavallo, *Top. Curr. Chem.,* 2011, **302**, 131; (*h*) *N-Heterocyclic Carbenes*, ed. S. Díez-González, Royal Society Chemistry, 2011; (*i*) L. Benhamou, E. Chardon, G. Lavigne, S. Bellemin-Laponnaz, V. César, *Chem. Rev.,* 2011,

Dalton Trans., 2016, 45, 561–571. doi: 10.1039/c5dt03758a

111, 2705; (*j*) M. Fevre, J. Pinaud, Y. Gnanou, J. Vignolle, D. Taton, *Chem. Soc. Rev.*, 2013, **42**, 2142.

3 (*a*) R. H. Grubbs, *Handbook of Metathesis*; Wiley-VCH: Weinheim, Germany, 2003; Vols. 1−3. (*b*) S. J. Connon, S. Blechert, In *Ruthenium Catalysts and Fine Chemistry*, eds. P. H. Dixneuf, C. Bruneau, Springer: Heidelberg, Germany, 2004; Vol. 11, p. 93; (*c*) A. Fürstner, *Angew. Chem*., 2000, **112**, 3140; *Angew. Chem., Int. Ed.*, 2000, **39**, 3012; (*d*) A. H. Hoveyda, A. R. Zhugralin, *Nature*, 2007, **450**, 243; (*e*) P. H. Deshmuhk, S. Blechert, *Dalton Trans.*, 2007, 2479; (*f*) D. Astruc, *New J. Chem.*, 2005, **29**, 42; (*g*) A. M. Lozano-Vila, S. Monsaert, A. Bajek, F. Verpoort, *Chem. Rev.*, 2010, **110**, 4865; (*h*) *Olefin Metathesis Theory and Practice*, ed. K. Grela, J. Wiley & Sons: Hoboken, NJ, 2014.

4 (*a*) G. C. Vougioukalakis, R. H. Grubbs, *Chem. Rev.*, 2010, **110**, 1746; (*b*) C. Samojlowicz, M. Bieniek, K. Grela, *Chem. Rev.*, 2009, **109**, 3708; (*c*) C. E. Diesendruck, E. Tzur, N. G. Lemcoff, *Eur. J. Inorg. Chem.*, 2009, 4185; (*d*) C. Fischmeister, P. H. Dixneuf, *Metathesis Chemistry: From Nanostructure Design to Synthesis of Advanced Materials*, eds. Y. Imamoglu, V. Dragutan, Springer: Dordrecht, The Netherlands, 2007, pp 3−27; (*e*) M. Bieniek, A. Michrowska, D. L. Usanov, K. Grela, *Chem. Eur. J.*, 2008, **14**, 806.

5 For asymmetric transformations, see: (*a*) R. E. Giudici, A. H. Hoveyda, *J. Am. Chem. Soc.*, 2007, **129**, 3824; (*b*) B. K. Keitz, R. H. Grubbs, *Organometallics*, 2010, **29**, 403; (*c*) B. Stenne, J. Timperio, J. Savoie, T. Dudding, S. K. Collins, *Org. Lett.*, 2010, **12**, 2032; (*d*) T. W. Funk, J. M. Berlin, R. H. Grubbs, *J. Am. Chem. Soc.*, 2006, **128**, 1840; (*e*) B. Schmidt, L. Staude, *J. Org. Chem.*, 2009, **74**, 9237; (f) S. Tiede, A. Berger, D. Schlesiger, D. Rost, A. Lühl, S. Blechert, *Angew. Chem., Int. Ed.*, 2010, **49**, 3972.

6 For sterically demanding reactions, see: (*a*) I. C. Stewart, T. Ung, A. A. Pletnev, J. M. Berlin, R. H. Grubbs, Y. Schrodi, *Org. Lett.*, 2007, **9**, 1589; (*b*) J. M. Berlin, K. Campbell, T. Ritter, T. W. Funk, A. Chlenov, R. H. Grubbs, *Org. Lett.*, 2007, **9**, 1339.

Dalton Trans., 2016, 45, 561–571. doi: 10.1039/c5dt03758a

7 For aqueous transformations, see: (*a*) S. J. Connon, S. Blechert, *Bioorg. Med. Chem. Lett.*, 2002, **12**, 1873; (*b*) L. Gulajski, A. Michrowska, R. Bujok, K. Grela, *J. Mol. Catal. A*, 2006, **254**, 118; (*c*) J. P. Jordan, R. H. Grubbs, *Angew. Chem., Int. Ed.*, 2007, **46**, 5152; (*d*) A. Michrowska, L. Gulajski, Z. Kaczmarska, K. Mennecke, A. Kirschning, K. Grela, *Green Chem.*, 2006, **8**, 685; (*e*) D. Burtscher, K. Grela, *Angew. Chem., Int. Ed.*, 2009, ***48***, 442; (*f*) S. H. Hong, R. H. Grubbs, *J. Am. Chem. Soc.*, 2006, **128**, 3508.

8 Representative examples: (*a*) T. J. Seiders, D. W. Ward, R. H. Grubbs, *Org. Lett.*, 2001, **3**, 3225; (*b*) T. Ritter, M. W. Day, R. H. Grubbs, *J. Am. Chem. Soc.*, 2006, **128**, 11768; (*c*) C. K. Chung, R. H. Grubbs, *Org. Lett.*, 2008, **10**, 2693; (*d*) K. M. Kuhn, J.-B. Bourg, C. K. Chung, S. C. Virgil, R. H. Grubbs, *J. Am. Chem. Soc.*, 2009, **131**, 5313; (*e*) T. Savoie, B. Stenne, S. K. Collins, *Adv. Synth. Catal.*, 2009, **351**, 1826; (*f*) M. Gatti, L. Vieille-Petit, X. Luan, R. Mariz, E. Drinkel, A. Linden, R. Dorta, *J. Am. Chem. Soc.*, 2009, **131**, 9498; (*g*) L. Vieille-Petit, X. Luan, M. Gatti, S. Blumentritt, A. Linden, H. Clavier, S. P. Nolan, R. Dorta, *Chem. Commun.*, 2009, 3783; (*h*) F. Grisi, C. Costabile, E. Gallo, A. Mariconda, C. Tedesco, P. Longo, *Organometallics*, 2008, **27**, 4649.

9 (*a*) J. Tornatzky, A. Kannenberg, S. Blechert, *Dalton Trans.*, 2012, **41**, 8215; (*b*) F. B. Hamad, T. Sun, S. Xiao, F.Verpoort, *Coord. Chem. Rev.*, 2013, **257**, 2274.

10 Selected examples of *N*-alkyl/*N*-aryl NHC-Ru complexes: (*a*) K. Vehlow, S. Maechling, S. Blechert, *Organometallics*, 2006, **25**, 25; (*b*) N. Ledoux, A. Linden, B. Allaert, H. V. Mierde, F. Verpoort, *Adv. Synth. Catal.*, 2007, **349**, 1692; (*c*) K. Vehlow, D. Wang, M. R. Buchmeiser, S. Blechert, *Angew. Chem., Int. Ed.*, 2008, **47**, 2615; (*d*) R. M. Thomas, B. K. Keitz, T. M. Champagne, R. H. Grubbs, *J. Am. Chem. Soc.*, 2011, **133**, 7490; (*e*) O. Ablialimov, M. Kedziorek, C. Toborg, M. Malinska, K. Wozniak, K. Grela, *Organometallics*, 2012, **31**, 7316; (*f*) O. Ablialimov, M. Kedziorek, M. Malinska, K. Wozniak, K. Grela, *Organometallics*, 2014, **33**, 2160; (*g*) M. Rouen, E. Borré, L. Falivene, L. Toupet, M. Berthod, L. Cavallo, H. Olivier-

Dalton Trans., 2016, 45, 561–571. doi: 10.1039/c5dt03758a

Bourbigou, M. Mauduit, *Dalton Trans.*, 2014, **43**, 7044; (*h*) B. Yu, F. B. Hamad, B. Sels, K. Van Hecked, F. Verpoort, *Dalton Trans.*, 2015, **44**, 11835.

11 K. Endo, R. H. Grubbs, *J. Am. Chem. Soc.*, 2011, **133**, 8525.

12 V. Paradiso, V. Bertolasi, F. Grisi, *Organometallics*, 2014, **33**, 5932.

13 (*a*) F. Grisi, A. Mariconda, C. Costabile, V. Bertolasi, P. Longo, *Organometallics*, 2009, **28**, 4988; (*b*) C. Costabile, A. Mariconda, L. Cavallo, P. Longo, V. Bertolasi, F. Ragone, F. Grisi, *Chem. Eur. J.*, 2011, **17**, 8618.

14 The stability of catalysts **7**-**10** was also monitored over time using 1,3,5-trimethoxybenzene as an internal standard. Experiments were performed, under nitrogen, at 30°C in CD_2Cl_2 for **7** and **8**, and at 60°C in C_6D_6 for **9** and **10**. After a week, only **7** was found fully decomposed.

15 Complex **7** showed a *syn:anti* ratio 0.3:1; while complex **8** a *syn:anti* ratio 0.8:1. Any attempt to separate these rotamers failed.

16 (*a*) S. K. Collins, P.-A. Fournier, *Organometallics*, 2007, **26**, 2945; (*b*) P.-A. Fournier, J. Savoie, M. Bédard, B. Stenne, A. Grandbois, S. K. Collins, *Chem. Eur. J.*, 2008, **14**, 8690; (*c*) B. Stenne, J. Timperio, J. Savoie, T. Dudding, S. K. Collins, *Org. Lett.*, 2010, 12, 2032.

17 This finding is in line with the results reported by Collins in ref.8e. The catalyst stability increases with increasing the size of the *N*-alkyl group.

18 A small amount of two minor carbenic species were detected in the ^{1}H NMR spectrum of complex **13**. However, due to their low abundance, identification was not possible.

19 Dichloro[1,3-bis(2-methylphenyl)-2-imidazolidinylidene](benzylidene) (tricyclohexylphosphine) ruthenium(II).

20 Dichloro[1,3-bis(2-methylphenyl)-2-imidazolidinylidene](2-isopropoxyphenylmethylene) ruthenium(II).

Dalton Trans., 2016, 45, 561–571. doi: 10.1039/c5dt03758a

21 See for example: (*a*) L. Vieille-Petit, H. Clavier, A. Linden, S. Blumentritt, S. P. Nolan, R. Dorta, *Organometallics*, 2010, **29**, 775; (b) A. Perfetto, C. Costabile, P. Longo, F. Grisi, *Organometallics*, 2014, **33**, 2747.

22 At 1 mol%, the reaction is complete in less than two minutes.

23 I. C. Stewart, B. K. Keitz, K. M. Kuhn, R. M. Thomas, R. H. Grubbs, *J. Am. Chem. Soc.*, 2010, **132**, 8534.

24 A. Perfetto, C. Costabile, P. Longo, V. Bertolasi, F. Grisi, *Chem. Eur. J.*, 2013, **19**, 10492.

25 (*a*) A. K. Chatterjee, T.-L. Choi, D. P. Sanders, R. H. Grubbs, *J. Am. Chem. Soc.*, 2003, **125**, 11360; (*b*) T. Ritter, A. Hejl, A. G. Wenzel, T. W. Funk, R. H. Grubbs, *Organometallics*, 2006, **25**, 5740.

26 (*a*) T. J. Seiders, D. W. Ward, R. H. Grubbs, *Org. Lett.*, 2001, **3**, 3225; (*b*) T. W. Funk, J. M. Berlin, R. H. Grubbs, *J. Am. Chem. Soc.*, 2006, **128**, 1840.

27 (*a*) D. G. Gillingham, A. H. Hoveyda, *Angew. Chem. Int. Ed.*, 2007, **46**, 3860; (*b*) K. Takao, H. Yasui, S. Yamamoto, D. Sasaki, S. Kawasaki, G. Watanabe, K. Tadano, *J. Org. Chem.*, 2004, **69**, 8789; (*c*) G. A. Cortez, R. R. Schrock, A. H. Hoveyda, *Angew. Chem. Int. Ed.*, 2007, **46**, 4534.

28 R. M. Thomas, R. H. Grubbs, *Chemistry in New Zealand,* 2011, **75**, 65.

29 (*a*) M. Iglesias, D. J. Beetstra, B. Kariuki, K. J. Cavell, A. Dervisi, I. A. Fallis, *Eur. J. Inorg. Chem.,* **2009**, 1913; (*b*) Y. Borguet, G. Zaragoza, A. Demonceau, L. Delaude, *Dalton Transactions*, 2015, **44**, 9744.

30 H. D. Flack, *Acta Crystallogr. Sect A,* 1983, **39**, 876.

31 M. N. Burnett, C. K. Johnson, ORTEP III, Report ORNL-6895, Oak Ridge National Laboratory, Oak Ridge, TN, 1996.

32 F. E. Hahn, M. Paas, D. Le Van, T. Lugger, *Angew. Chem. Int. Ed.,* 2003, **42**, 5243.

Dalton Trans., 2016, 45, 561–571. doi: 10.1039/c5dt03758a

33 M. Alcarazo, S. J. Roseblade, E. Alonso, R. Fernandez, E. Alvarez, F. J. Lahoz, J. M. Lassaletta, *J. Am. Chem. Soc.* 2004, **126**, 13242.

34 E. Jansen, M. Lutz, B. de Bruin, C. J. Elsevier, *Organometallics*, 2014, **33**, 2853.

35 C. Mejuto, G. Guisado-Barrios, E. Peris, *Organometallics*, 2014, **33**, 3205.

36 A. Poater, B. Cosenza, A Correa, S. Giudice, F. Ragone, V. Scarano, L. Cavallo, *Eur. J. Inorg. Chem.* 2009, 1759. The default processing parameters of Samb*V*ca web application were kept unchanged.

37 The $\%V_{Bur}$ values for the same NHC ligands where calculated also using the crystal structures of **9** and **10**, reported in ref.12, and they were found to be 29.9 for *syn*-uNHC and 29.1/29.4 for *anti*-uNHC (considering the two independent molecules of **10**).

38 T. Dröge, F. Glorius, *Angew. Chem. Int. Ed.* 2010, **49**, 6940.

Dalton Trans., 2016, 45, 561–571. doi: 10.1039/c5dt03758a

Graphical content

Ruthenium Olefin Metathesis Catalysts Featuring Unsymmetrical N-Heterocyclic Carbenes

Veronica Paradiso, Valerio Bertolasi, Chiara Costabile and Fabia Grisi*